Does "Birth" as an Event Impact Maturation Trajectory of Renal Clearance via Glomerular Filtration? Reexamining Data in Preterm and Full-Term Neonates by Avoiding the Creatinine Bias

Farzaneh Salem, PharmD, PhD[1], Trevor N. Johnson, PhD[1], Arran B. J. Hodgkinson, PhD[1], Kayode Ogungbenro, PhD[2], and Amin Rostami-Hodjegan, PharmD, PhD, FCP[1,2]

Abstract

Glomerular filtration rate (GFR) is an important measure of renal function. Various models for its maturation have recently been compared; however, these have used markers, which are subject to different renal elimination processes. Inulin clearance data (a purer probe of GFR) collected from the literature were used to determine age-related changes in GFR aspects of renal drug excretion in pediatrics. An ontogeny model was derived using a best-fit model with various combinations of covariates such as postnatal age, gestational age at birth, and body weight. The model was applied to the prediction of systemic clearance of amikacin, gentamicin, vancomycin, and gadobutrol. During neonatal life, GFR increased as a function of both gestational age at birth and postnatal age, hence implying an impact of birth and a discrepancy in GFR for neonates with the same postmenstrual age depending on gestational age at birth (ie, neonates who were outside the womb longer had higher GFR, on average). The difference in GFR between pre-term and full-term neonates with the same postmenstrual age was negligible from beyond 1.25 years. Considering both postnatal age and gestational age at birth in GFR ontogeny models is important because postmenstrual age alone ignores the impact of birth. Most GFR models use covariates of body size in addition to age. Therefore, prediction from these models will also depend on the change in anthropometric characteristics with age. The latter may not be similar in various ethnic groups, and this makes the head-to-head comparison of models very challenging.

The glomerular filtration rate (GFR) is an important marker of renal function. There are several published models that estimate GFR based on the clearance of endogenous (creatinine) or exogenous (eg, mannitol, iohexol, inulin, and aminoglycosides) compounds. Nonlinear mixed-effects modeling of renally cleared drugs such as amikacin,[1-3] gentamicin,[4-9] and vancomycin[10] is often used to show the development of renal function in pediatrics.[11] This approach predominantly uses age as either "postnatal age," "gestational age at birth," "postconceptional" or "postmenstrual age"[12-14] combined with body weight (BW) as significant covariates in population pharmacokinetic (PopPK) models. However, using age in the form of postmenstrual age or postconceptional age alone in these models undermines the effect of birth on the development of renal function. A number of PopPK models proposed postnatal age, gestational age at birth, and BW as ideal covariate candidates to reflect the rapid development of GFR in the first few days after birth. The scope of these models, however, is limited to specific drugs.[9,10,15-17]

Serum creatinine has been historically used as a marker of renal function in the clinic because of its ease of measurement. Recent in vitro and in vivo studies, however, suggest involvement of active processes beyond glomerular filtration via transporters, such as organic cation transporter (OCT) 2,[18,19] OCT3,[20]

[1]Certara UK Ltd, Simcyp Division, Sheffield, UK
[2]Centre for Applied Pharmacokinetic Research, Division of Pharmacy and Optometry, School of Health Sciences, Faculty of Biology, Medicine and Health, Manchester Academic Health Science Centre, University of Manchester, Manchester, UK

Corresponding Author:
Farzaneh Salem, PharmD, PhD, Certara UK Ltd, Simcyp Division, Level 2-Acero, 1 Concourse Way, Sheffield, S1 2BJ, UK
Email: Farzaneh.Salem@Certara.com

organic anion transporter (OAT)2,[21] multidrug and toxin extrusion protein (MATE) 1, and MATE2-K.[22-24] Recently, Cheung et al[25] and Li et al[26] reported the ontogeny of several renal transporters and showed that expression of OCT2 but not MATE1 and MATE2-K increased with age. Because expression and activity of the transporters involved in active tubular secretion of creatinine could change with age, which may not necessarily be in parallel with maturation of the filtration mechanism, it is likely that the GFR measurements based on serum creatinine are influenced by age-related changes in transporter protein expression. Hence, the use of such clearance values as an indication of GFR could be misleading. To overcome this problem, a pure marker of GFR is required that only reflects filtration in nephrons. Among the substrates used for the measurement of GFR, the clearance of inulin is regarded as the "gold standard."[27]

The GFR can be predicted from different models reported in the literature. Direct comparison of models in the form of renal function versus age, however, is challenging, especially if the measures related to "size" were not similar as an input covariate. Thus, the relative prediction of these models (for average renal function vs age) will change depending on the population and associated body size with age.[11,14,28,29]

There are multiple aims in the current study, but the most important aims are:

- To reexamine the ontogeny function for GFR maturation, using inulin clearance as a purer and more accurate marker of GFR, which avoids the aforementioned issues with transporter ontogeny.
- To determine the impact of birth as a step change on GFR maturation in preterm and full-term neonates. To distinguish the GFR changes associated with prenatal and postnatal age, we have used gestational age at birth, postnatal age, and BW as covariates in the model to show whether, for a fixed postmenstrual age, subjects born more preterm may have a higher GFR. This may have clinical implications in calculating the appropriate drug dose administered to infants with the same postmenstrual age but different postnatal age and vice versa.
- To examine application of this model for the prediction of systemic clearance for renally cleared drugs.
- To explore the comparison between different models when input parameters into the models are different.

Methods

Literature Search and Compilation of Database

The literature was searched for studies that reported inulin systemic clearance values after intravenous infusion covering the whole pediatric age range and young adults from newborn to 25 years. Data were retrieved from PubMed and Google Scholar searches. Key words, in addition to inulin, were "clearance," in combinations with "pediatric," "neonate," "infant," "children," "adults," or "subject." All the articles retrieved were screened for relevance and the reference lists scanned to identify other applicable articles. Studies that report renal clearance of inulin at steady state during a constant intravenous infusion were included, but single-administration studies were excluded. In particular, information on the body weight, height, body surface area (BSA), postnatal age, gestational age at birth, postmenstrual age, and numbers of subjects was extracted. Inulin clearance (GFR) values from these studies were transformed to absolute values in units of milliliters per minute from the originally reported units using reported or calculated BSA, as discussed in the following sections. Absolute clearance values (mL/min) were normalized by the mean inulin clearance value (114.3 mL/min) in healthy adult volunteers (age, 18-25 years; mean BW, 79.4 kg; mean BSA, 1.97 m^2) to generate the fraction of adult values across the whole pediatric population. Details of all inulin studies are presented in Table S1 in the Appendix. Where possible, individual values of intravenous inulin clearance were used. Where individual values were not available, however, bootstrapping was carried out to generate individual values of age parameters (gestational age at birth or postnatal age) and CL (mL/min or mL/min/m^2). The flow diagram in the supplementary material (Figure S1) presents the methodology to arrive at final individual age and inulin clearance values (mL/min). For age parameters, reported minimum and maximum values in the references were used to perform random sampling from a uniform distribution, as described in the next section. Where minimum and maximum values were not available, reported mean and standard deviation values were used to arrive at minimum and maximum values using equation 1 and equation 2.

$$Age_{min} = Age_{Mean} - (2 \times SD) \qquad (1)$$

$$Age_{max} = Age_{Mean} + (2 \times SD) \qquad (2)$$

where Age_{min} and Age_{max} are minimum and maximum values of postnatal age or gestational age at birth in the study and Age_{Mean} and standard deviation (SD) are the reported mean and SD in that study for postnatal age or gestational age at birth.

In this approach, assuming a normal distribution, 95% of age values fall within 2 SD around the mean, and therefore minimum and maximum values of age parameters are estimated from equation 1 and equation 2.

For clearance values, random sampling was carried out from a normal distribution. Bootstrapping and random generation of individual values for postnatal

age, gestational age at birth, and GFR are discussed in the following section.

Bootstrapping, Random Number Generation, and Unit Transformation

Bootstrapping was carried out in Microsoft Office Excel to generate individual inulin clearance, gestational age at birth, and postnatal age values from the reported mean and SD or the calculated range of these parameters, where individual values were not reported within the references. This allowed us to generate individual values from a clinical study and facilitated weighting for the number of subjects during the model-fitting stage. This also allowed us to account for the variability of age and clearance in those studies.

Random sampling for age parameters was performed from a uniform distribution in Microsoft Office Excel using the Mersenne Twister algorithm (MT19937) based on minimum and maximum values of parameters (equation 3).

$$Age_i = Age_{min} + RAND() \times (Age_{max} - Age_{min}) \quad (3)$$

where Age_i, Age_{min}, and Age_{max} are the individual's age (postnatal age), minimum and maximum age values reported in the article or calculated from equations 1 and 2 and RAND() is an Excel function for random number generation. For reported mean and SD values in clinical studies, equation 1 and equation 2 were used to calculate the minimum and maximum values, and then equation 3 was used to generate individual values. In full-term neonates, if there were no information on gestational age at birth, minimum and maximum values of 37 and 42 weeks were assumed.

For inulin clearance, reported mean and standard deviation from the studies were used to generate a normal distribution for the number of subjects in that report in Microsoft Office Excel using the NORMINV(rand(), mean, SD) function. Normal distribution (NORMINV function in Excel) was used to generate inulin clearance values normalized per BSA. Sampling was repeated if negative clearance values were generated. If the age range of subjects was reasonably narrow (ie, a few days in neonates) or in adults, in whom significant age-related changes in demographics were not expected, only random number generation (uniform distribution) was used to produce individual clearance values.

If the reported or generated clearance values were in units of mL/min/1.73 m^2 or mL/min/m^2, BSA was used to transform the units of GFR to mL/min. For calculation of BSA, male height and weight relationships in equation 4 to equation 7 were used. Full-term height and BW relationships were based on our in-house analysis based on data from UK 1996 growth charts (equations 4 and 5). For preterm neonates, equations from Abduljalil et al[30] were used (equations 6 and 7).

$$Height = 0.0000176179 \times Age^7 - 0.00119874 \times Age^6$$
$$+ 0.0323848 \times Age^5 - 0.444112 \times Age^4$$
$$+ 3.2946 \times Age^3 - 13.2191$$
$$\times Age^2 + 33.75 \times Age + 52.62152 \quad (4)$$

$$Body\ weight = 7.826 \times (1.0 - exp(Age \times -1.2))$$
$$+ exp((Height \times 0.0209) + (0.023 \times Age)) \quad (5)$$

where Age is in years, BW is in kilograms, and height is in centimeters.

$$Height = -43.205 \times PMA^2$$
$$+ 111.84 \times PMA - 9.4871 \quad (6)$$

$$Weight = PMA \times (0.0373 \times Height)^{2.36} \quad (7)$$

where postmenstrual age is measured in years.[30]

Where BW and height were calculated from the above equations, an additional fixed CV (coefficient of variation) = 15% for BW and CV = 6% for height based on in-house analysis were applied to these parameters before being used in BSA calculations. In full-term neonates, the BSA calculation was done using Haycock et al[31] for BW below 15 kg and Du Bois and Du Bois[32] for BW over 15 kg, the modified Meban equation was used in preterm neonates.[30,33]

Model Building

A variety of models (exponential, linear, sigmoid, Gompertz, and polynomial functions) were assessed in Phoenix 7.0.0.2535 to obtain the best fit to the clinical data. To avoid weighting for the size of clinical study and at the same time benefit from the variability of data, the reported individual or bootstrapped data were included in the analysis. Body weight ratio (R_{BW}, ratio of present body weight relative to adult BW of 79.4 kg), BSA ratio (ratio of present body surface area relative to adult body surface area of 1.97 m^2), postnatal age, and gestational age at birth were tested as covariates in the model. The information on these covariates was provided in the majority of studies.

The best model fit from mathematical functions was selected based on minimum −2LL and the uncertainty (CV) on the estimated parameters; these functions are presented below.

$$GFR\ Ratio\ 1 = 0.01 + exp(P_{2\times}(GA_B - 25)) \times R_{Bw}^{P3} \quad (8)$$

$$\text{GFR Ratio } 2 = \Bigg[\big(P_4 - (0.01 + \exp(P_{2\times}(GA_B - 25)))$$

$$\times R_{Bw}^{P3})\big) \times \frac{PNA^{P5}}{P6^{P5} + PNA^{P5}}$$

$$+ \big(0.01 + \exp(P_{2\times}(GA_B - 25))$$

$$\times R_{Bw}^{P3}\big) \Bigg] \times R_{Bw}^{P10} \qquad (9)$$

$$\text{GFR Ratio } 3 = \Bigg[\big(P_4 - (0.01 + \exp(P_{2\times}(GA_B - 25)))$$

$$\times R_{Bw}^{P3})\big) \times \frac{PNA^{P5}}{P6^{P5} + PNA^{P5}}$$

$$+ \big(0.01 + \exp(P_{2\times}(GA_B - 25)) \times R_{Bw}^{P3}\big) \Bigg]$$

$$\times R_{Bw}^{P10} + P_7 \times \exp(P_8 \times (PNA - P_9))$$

$$(10)$$

where GA_B is gestational age at birth, PNA is postnatal age, and R_{BW} is the ratio of individual body weight to the average adult body weight of 79.42 kg. The parameters in the equations above were P_1, a fixed fraction of the GFR value for viable neonates if born before 25 weeks' gestational age; P_2, the rate of the GFR increase during gestational age; P_3, the allometric exponent; P_4, the maximum GFR ratio value between birth and 10 years; P_5, the sigmoidicity factor showing how fast maximum level is reached; P_6 (in weeks), the age at which half-maximum value was reached before 10 years; P_7, the additional baseline; P_8, the rate of GFR increase after 10 years; P_9 (in weeks), the age for switch between postnatal models; and P_{10}, the allometric exponent.

Because there were no subjects born before 25 gestational weeks in this analysis, the value for P_1 was fixed at a GFR ratio of 0.01 (1% adult GFR). This value was derived based on average GFR ratios from 16 neonates less than 1 day old as a postnatal age and born between 27 and 30 weeks of gestation. This value was also estimated during the fitting exercise, and a similar value of 0.01 was obtained.

If postnatal age was zero (at birth), GFR ratio 1 (equation 8), if postnatal age was less than 10 years (P_9, 10 years), GFR ratio 2 (equation 9), and if postnatal age was equal or greater than 10 years, GFR ratio 3 (equation 10) will be used to predict inulin clearance.

Equation 8 describes the model for GFR value at birth according to gestational age at birth and BW ratio. Equation 9 and equation 10 predict the GFR value after birth depending on postnatal age (weeks) and BW ratio. Equation 10 predicts GFR using postnatal age until 25 years. The switch between equation 9 and equation 10 (P_9) occurs based on a floating cutoff that is automatically estimated during the fitting exercise in Phoenix.

Model Application

The GFR model was developed based on all the retrieved inulin clearance data from the literature. This model was applied to predict clearance values (mL/min) of renally cleared drugs amikacin, gentamicin, vancomycin, and gadobutrol in different age groups. The clinical studies reporting amikacin, gentamicin, vancomycin, and gadobutrol were identified with the same methodology as described for inulin clearance. These data are presented in Tables S2-S5. Amikacin, gentamicin, vancomycin, and gadobutrol clearance values (mL/min) were predicted using equation 11:

$$CL_{Predicted} = CL_{Adult} \times Ontgeny\ function \qquad (11)$$

where $CL_{predicted}$ is the amikacin, gentamicin, vancomycin, and gadobutrol clearance (mL/min) predicted in different pediatric studies, CL_{adult} is the mean adult value of CL (mL/min) for these drugs based on meta-analysis of data from adult sepsis patients with normal renal function and ontogeny function is the prediction from inulin model for that age. Adult clearance values for these drugs from a meta-analysis of studies in patients with infection were 93.9 ± 37.9 and 89.8 ± 39.3 mL/min for gentamicin[34,35] and vancomycin (elderly subjects excluded),[36] respectively. Amikacin clearance for healthy subjects was 97.3 ± 15.0 mL/min.[37,38] Vancomycin pediatric data used in this comparison were from those studies that measured or monitored a patient's renal function during the course of therapy to avoid nephrotoxicity.

Predicted versus observed clearance was plotted, and 2-fold intervals were used to evaluate the predictions on a logarithmic scale. Assuming the constant CV between adults (CL_{adult}) and pediatrics, standard deviations on pediatric predictions ($CL_{predicted}$) were calculated and added to the graph. The standard deviation from the observed data was also added to the graph where possible.

Prospective Prediction

The difference in GFR between preterm and full-term neonates is expected to disappear later during postnatal age. The inulin model was used to predict postmenstrual age (in weeks) at which the difference in GFR between preterm and full-term neonates is less than 5%. For this purpose GFR fractions were predicted at gestational ages at birth of 25, 28, 31, 34, and 40 weeks and at fixed postmenstrual age of 32, 37, 40, and 105 weeks. The pattern of GFR development

for these gestational ages at birth was established. The reason for selecting these gestational ages at birth was to use the appropriate BW and height relationships based on postnatal age and gestational age at birth provided in the literature,[39] instead of using the general post-menstrual age-based equations that were used in inulin model building. The equations reported by Troutman et al[39] allowed generation of BW and height at different postnatal ages for the given gestational age at birth. Unfortunately, these relationships are only limited to certain gestational ages at birth and hence could not be applied in the inulin model-building process.

Comparison of Models

The GFR predictions by some of the models reported in the literature (Johnson, 2006; Rhodin, 2009 [empirical model]; De Cock et al, 2014; and Wang, 2019 [PNA-GA])[11,29] were compared with the current model and between themselves. In this comparison, average BW and height changes with age for male children were extracted from Japanese and Dutch growth charts and used as input into the models (either directly as BW or after combining with average height to give BSA). The predicted average GFR values for each country were plotted against age. The equations applied in this comparison include:

$$GFR = (-6.1604 \times BSA^2) + (99.054 \times BSA)$$
$$- 17.74 \quad \text{Johnson 2006}$$

$$GFR = \left(\frac{BW}{70}\right)^{0.632} \times \frac{PMA^{3.33}}{55.4^{3.33} \times PMA^{3.33}}$$
$$\times 112 \quad \text{Rhodin 2009}$$

$$GFR = CL_{GFR} \times \left(\frac{BW}{4}\right)^{BDE} \quad \text{and}$$
$$BDE = 2.23 \times BW^{-0.065} \quad \text{De Cock 2014}$$

$$GFR = \left(\frac{BW}{70}\right)^{0.75} \times (1 - (0.404 \times \left(\frac{GA_B}{37}\right)^{3.3}$$
$$\times \exp\left(-PNA \times \left(\frac{0.693}{20.8}\right)\right)) \times 121 \quad \text{Wang 2019.}$$

The Wang model uses the compound adult clearance value. In this case, the value of 121 mL/min based on the Rhodin (2009) theoretical model is applied to the Wang equation assuming normal renal function in all subjects.

Results

Literature Search and Compilation of Database

Fifteen clinical studies, 688 subjects in total, reporting intravenous inulin clearance data were included in the analysis. Table S1 in the Appendix presents the details of the clinical studies used in this analysis. The reported individual inulin clearance values were used as a fraction of the adult mean inulin clearance value of 114.3 mL/min from 38 adult subjects 18 to 25 years[40-42] in the analysis.

Model Building

An ontogeny model consisting of 3 functions was derived using the best-fit models for GFR values relative to the mean adult inulin clearance (114.3 mL/min) versus age. Estimated model parameters are presented in Table 1. Three covariates including gestational age at birth, postnatal age, and BW ratio were used in the model. Body weight ratio in combination with gestational age at birth significantly ($P < .05$) decreased $-2LL$ and improved the model-predicted GFR values at birth and during postnatal age. Table S6 in the Appendix compares the $-2LL$ values for different tested models.

Figure 1A shows the inulin clearance values for 147 subjects from birth to 1-day-old for full-term and preterm newborns and the fitted line from GFR ratio 1 (equation 8). Subjects reported to be born within minutes and hours up to 1 day were included here (postnatal age ≤1 day). This model provides the baseline GFR value at birth for neonates born after 25 weeks of gestation (lowest reported gestational age at birth in the data set). GFR at birth increases as a function of gestational age at birth and BW ratio. The exponential line shows the best-fit model based on $-2LL$. The body weight ratio is calculated in this model as the fraction of adult average body weight. Figure 1B shows the predicted versus observed GFR ratios and the 2-fold intervals around the line of unity.

In neonates older than 1 day postnatal age, infants, children, and adults, a Hill (279 subjects), and Hill combined with an exponential (137 subjects) model was used to account for postnatal age and BW ratio. Figure 2 presents the age-related changes in fraction of GFR as a function of postnatal age and R_{BW}. Figure 2A,B shows that the development of GFR values is in agreement at older ages when postnatal and postmenstrual age are almost the same. Figure 2C,D demonstrates different GFR developmental patterns in subjects younger than 45 weeks PMA. Subjects in Figure 2C are preterm and full-term neonates, but subjects in Figure 2D are neonates and infants depending on their gestational age at birth. Postnatal age (Figure 2C) will provide a different picture compared with

Table 1. Parameter Values for the Final GFR Model and Uncertainty Around the Estimated Parameters

Parameter	Estimated	Standard Error	CV%	Definition
P_1[a]	0.009	0.001	40	A fixed fraction of GFR value for viable neonates if born before 25 weeks GA_B
P_2	0.039	0.03	84	Rate of GFR increase during gestational age
P_3	1.434	0.20	14	Allometric exponent
P_4	0.546	0.06	12	Maximum GFR ratio value between birth and 10 years
P_5	0.481	0.06	12	Sigmoidicity factor shows how fast maximum level is reached
P_6 (weeks)	7.200	5.39	75	Age at which half-maximum value is reached before 10 years
P_7	0.051	0.02	44	
P_8	0.003	0.0004	15	Rate of GFR increase after 10 years
P_9 (weeks)[b]	519.857	0.31	0.1	Age for switch between PNA models
P_{10}	0.379	0.09	24	Allometric exponent

GFR Ratio $1 = 0.01 + \exp(P_{2\times}(GA_B - 25)) \times R_{Bw}^{P3}$

GFR Ratio $2 = (((P_4 - \text{GFR Ratio 1}) \times \frac{PNA^{P5}}{P6^{P5}+PNA^{P5}}) + \text{GFR Ratio 1}) \times R_{BW}^{P10}$

GFR Ratio $3 = \text{GFR Ratio 2} + P_7 \times \exp(P_8 \times (PNA - P_9))$

[a] P1 the values for P1 are the mean, CV, and SE of GFR ratios for 16 less than 1-day neonates born between 27 and 30 GAB week to show the variability on this parameter.

[b] P9 is 10 years.
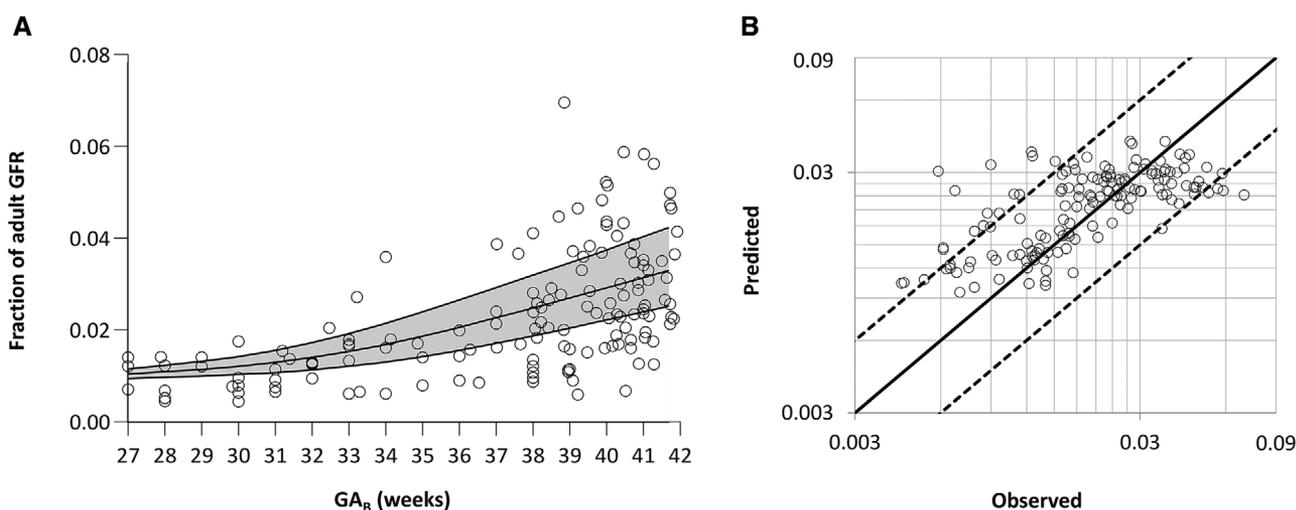
Figure 1. Fraction of adult GFR at birth increases with gestational age. The model predicts neonatal GFR as a fraction of the adult value (values in mL/min, not normalized for body size), at birth in preterm and full-term neonates based on the gestational age at birth and body weight ratio. (A) GFR ratio in neonates born with median body weight (50th centile) at different gestational ages. Gray area shows this model predictions for neonates born with body weight within the 2nd and 98th centiles. (B) Predicted versus observed GFR ratios. The solid line is the line of unity, and broken lines are 2-fold intervals around the line of unity. The observed data and references are reported in Table S1 of the supplementary material.

postmenstrual age between 25 and 45 weeks (Figure 2D). Including postnatal age and gestational age at birth in the baseline model enabled the impact of birth at a specific gestational age to be taken into account, which could not be considered based solely on using either gestational age at birth, postnatal age, or postmenstrual age alone.

The left-hand panel in Figure 3 shows that for neonates with similar postmenstrual age, babies with lower gestational age at birth will have higher GFR values compared with neonates of the same postmenstrual age who were born more mature (ie, effect of being outside the womb). In additional to having different GFR values at birth (based on their gestational age

at birth and BW), neonates will show different GFR values for a given postmenstrual age compared with those born at different gestational ages. These differences tend to disappear from about 1.25 years postnatal age (105 weeks' postmenstrual age). The right panel in Figure 3 shows the same information from a different angle. Figure 3 shows postmenstrual age at various gestational ages at birth, highlighting that the effect of birth (being premature or mature) certainly disappears by postmenstrual age of 105 weeks.

Model Application

Figure 4 shows the model predictions when applied to predict clearance for amikacin, gentamicin,
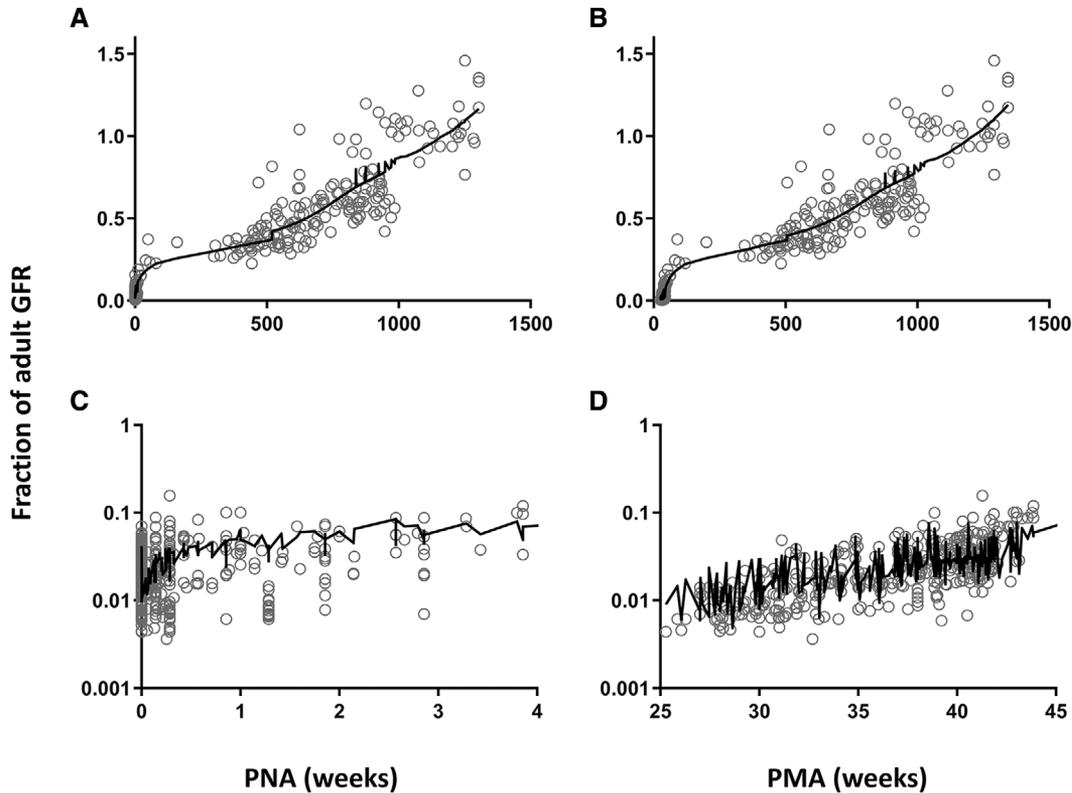
Figure 2. Fraction of adult GFR value from birth across the whole age range (values in mL/min, not normalized for body size). (A) Fraction of GFR versus postnatal age after birth until 25 years. (B) Fraction of GFR versus PMA until 25 years. (C) First 4 weeks of postnatal age from (A). (D) First few postmenstrual age weeks for subjects younger than 45 postmenstrual weeks. Gray circles represent observed in vivo data as a fraction of GFR values at each age relative to the mean adult reference value (114.3 mL/min). The black solid line is the best-fit models to the observed ratios. Observed data are from the clinical studies reported in Table S1. The values of 500 and 1000 PNA weeks correspond to 9.6 and 19.2 years, respectively. (A) and (B) are in agreement at higher ages, when postnatal and postmenstrual ages are almost the same. The observed data and associated references are reported in Table S1 of the supplementary material.

vancomycin, and gadobutrol in different age groups versus observed data. The horizontal error bars show standard deviation on observed data (where reported), and vertical error bars show standard deviation for predictions based on adult CV. Figure 4 shows a systematic departure in preterm neonates for amikacin, vancomycin, and gentamicin. Predictions for gadobutrol in children are in close agreement with inulin clearance. Although the data are limited in some age groups, the overall trend shows improvement in predictions with increasing age.

Comparison of Models
Body surface area (BSA) increases with age at different rates in children from different countries. At a certain age, children from different ethnicities may have different BSAs (Figure 5). In general, Dutch and Japanese children have the highest and lowest BSAs; however, the difference between nationalities is not linear in each age group. Japanese children have the lowest BSA at birth but, at certain times during infancy, have a higher BSA compared with children from China and Saudi

Arabia. Figure 6 shows predicted average GFR values for pediatric subjects using models by Johnson et al[28], Rhodin et al[24], an empirical model, De Cock et al[11], and Wang et al[29], maturation (GA, PNA) model. Figure 6 shows that the relative pattern of GFR with age in models is dependent on the anthropometric measures used to inform the models (Japanese [A, B, and C] versus Dutch [D, E, and F] in this case).

Discussion
As opposed to focusing on any specific drug, understanding the ontogeny of various aspects of renal function can enable prediction of renal clearance in different pediatric populations for any drug. To achieve this, the specific attributes associated with a particular drug can be related to aspects of renal function and predicted over time.

Creatinine clearance is commonly used as a measure of GFR after accounting for the endogenous production rate and its covariates (such as age, sex, and weight). In studies in mice, however, estimated values

A

B
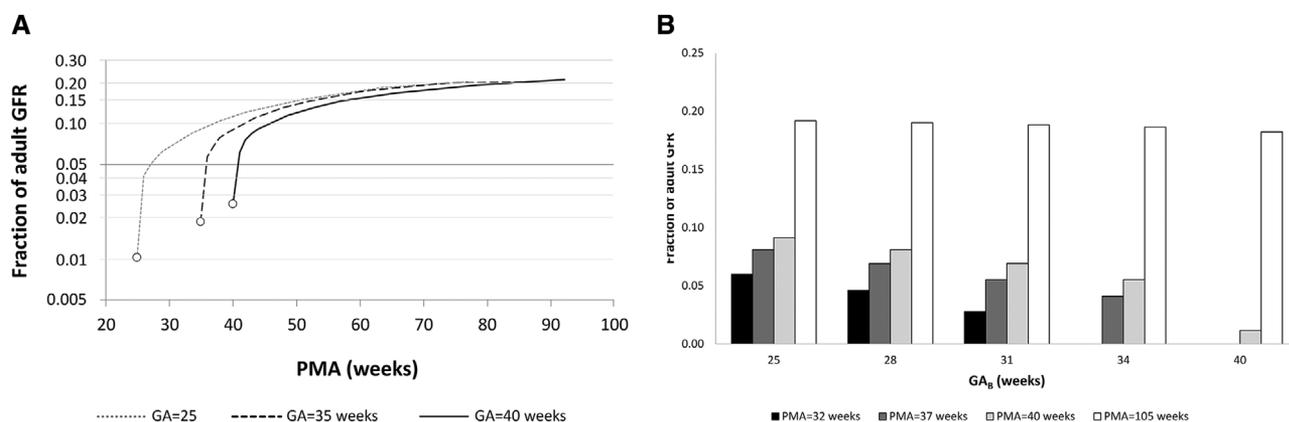
Figure 3. Simulated GFR development from birth using different gestational ages at birth (A). The lines and associated symbols present the pattern of GFR development from birth onward with postmenstrual age (weeks) for the given gestational age at birth. The circles indicate the GFR value at birth for the given gestational age. Please note the y axis is on a logarithmic scale. Effects of increasing postmenstrual age on the GFR (B) as a ratio of adult absolute value (mL/min) and not normalized for size in premature neonates of varying gestational ages at birth.

using creatinine clearance were higher compared with simultaneous inulin clearance using bolus and infusion methods.[43,44] In a study in healthy volunteers, measured inulin and creatinine clearance values were 105 and 117 mL/min, respectively.[45] A comparison of creatinine with inulin clearance ratios in adults, children, and neonates showed that, in general, the ratios are more than 1 in adults and below or close to 1 in the pediatric age groups.[45-48] Although these authors have applied different methodologies, the results indicate creatinine compared with inulin is excreted via additional mechanisms that may not be fully developed in young subjects. Recently the complexity of creatinine renal clearance and the involvement of several transporters have been highlighted.[22,23] Therefore, measured serum creatinine clearance is the net effect of both filtration and active tubular secretion. The latter can be affected by changes in the activity of transporters and therefore confound the prediction of GFR based on serum creatinine.

This model was developed using inulin data, which is considered the "gold standard" measure of GFR, to avoid the risk of "contamination" of results because of active tubular secretion or reabsorption. The main aim was to investigate the effect of birth as a step change on maturation of GFR. Birth is associated with complex physiological changes to the cardiovascular, respiratory, hematologic, central nervous, endocrine, gastrointestinal, and renal systems in the newborn. The latter includes increase in renal blood and reduction in vascular resistance and increased urine output. All these are likely to affect neonatal GFR, both during birth and following umbilical cord clamping for the subsequent hours and weeks.[49-51] The model illustrates that for a given postmenstrual age (weeks), neonates born earlier (more preterm) have a higher GFR value, suggesting faster ontogeny and/or a step change in

GFR maturation when the baby is outside the womb. This increase in GFR seems to be an adaptation mechanism and follows the events that occurred after birth and therefore are considered similar in all neonates. The GFR difference does not persist between preterm and full-term and tends to disappear beyond postmenstrual age of 105 weeks (1.25 years of age), regardless of gestational age at birth. Our model shows that the absolute GFR (mL/min) reaches the half-maximal value (54.8 mL/min) at about 12.5 years.

Assuming all neonates less that 1 day old are "just born," a relationship between GFR at birth and gestational age at birth was established. Each subject takes the GFR at birth as a baseline and develops GFR with postnatal age. In this way, the subjects have a different starting GFR baseline depending on how mature they are. If only postmenstrual age were used, however, this difference could not be identified.

The covariates tested in model building were limited to age, BW, and BSA, whereas others such as Apgar score and critical illness may play a role in GFR but, because of lack of available information for all individuals, could not be tested in the current study.

Because the demographic data were not reported for all subjects, bootstrapping and sampling techniques were used, and some of demographic parameters were predicted. The age was generated by uniform distribution and then height, BW, and BSA were calculated based on the currently available relationships for average male pediatric subjects. All the above could have contributed to a large estimation error associated with P_2 (rate of GFR increase during gestational age) and P_6 (age at which half-maximum value is reached before 10 years). It is important to recall that error estimates for model parameters may not necessarily be independent from one another and may reflect variance
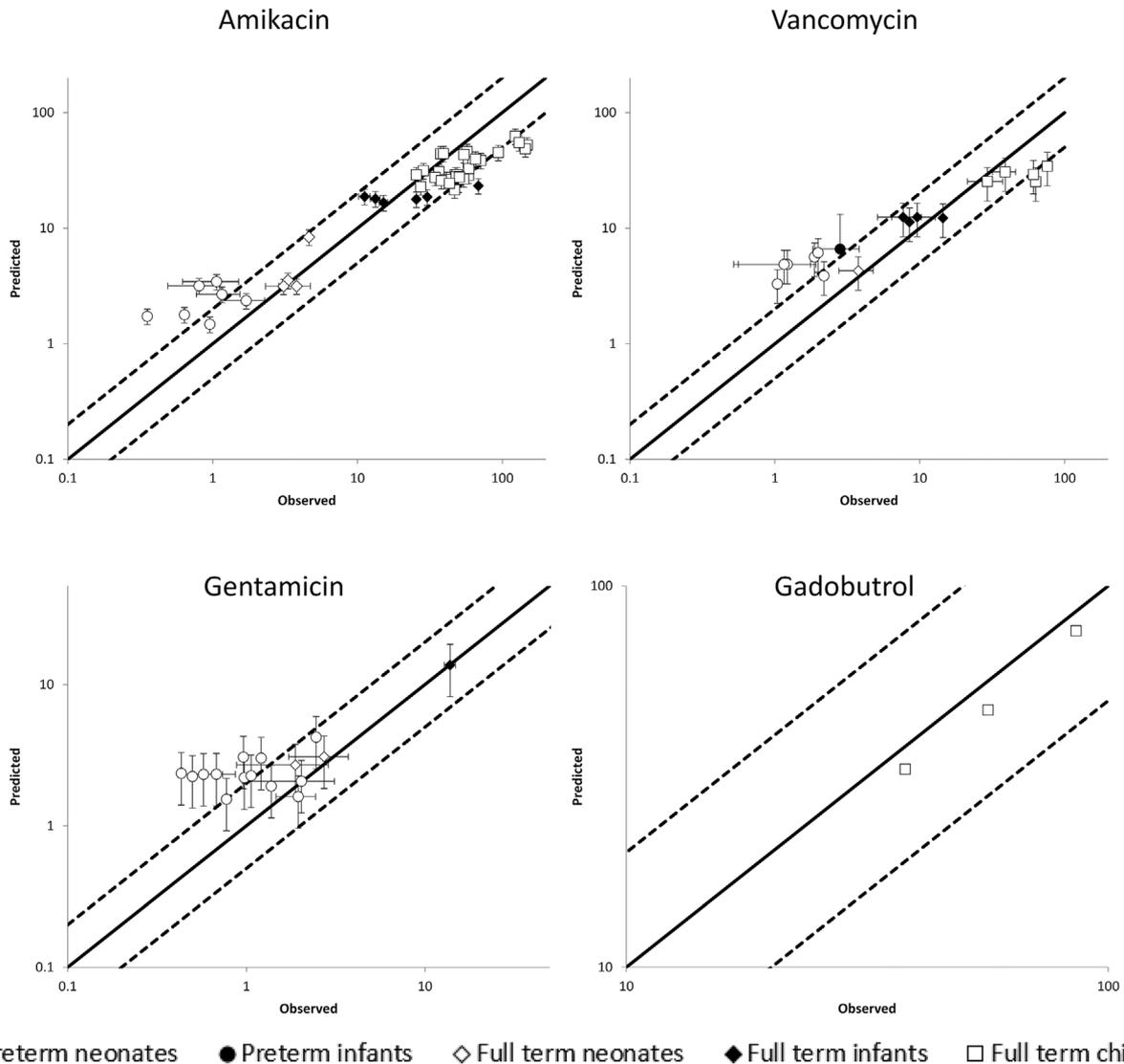
Figure 4. Predicted and observed CL values for gentamicin, amikacin, vancomycin, and gadobutrol. Solid line is line of unity, and dashed lines are 2-fold intervals. Observed data for these drugs are presented in Table S3 to Table S6.

within the data set itself, whereas observing appropriate covariance in parameters will retain goodness of fit.

Application of the inulin model to predominantly renally cleared drugs shows a systematic departure of clearance in preterm neonates. This observation is consistent with lower than 1 ratio of creatinine, the inulin ratio reported in newborns and infants.[46,47] This overprediction might indicate the contribution of other mechanisms involved in elimination of these drugs that develop at various rates in the preterm group. The information on ontogeny of some transporters has recently been published with some mRNA data in the preterm, but there is a need for more data in this area.[25] It is important that drugs used for application of the model are predominantly eliminated by GFR, with minimal contribution from other processes. There

is incomplete evidence to confirm lack of involvement of all renal transporters for all drugs applied to the current model, and hence, all the intravenous systemic clearance is attributed to GFR. Some data show vancomycin is cleared through renal excretion as well as nonrenal pathways including biliary excretion.[52,53] Renal excretion was reported to be 89% in healthy volunteers by Golper et al.[45] Vancomycin is reabsorbed from kidney tubules by megalin receptors.[54,55] Drug interaction studies in rat showed lack of interaction with probenecid (OAT1) and nonsignificant interactions with cimetidine (MATEs and OCT2) and quinidine (P-glycoprotein).[56] In rabbit kidney tubules, vancomycin is actively secreted.[57,58] For amikacin and gentamicin, there is some evidence of secretion and reabsorption.[59-61] Gadobutrol is suggested as the
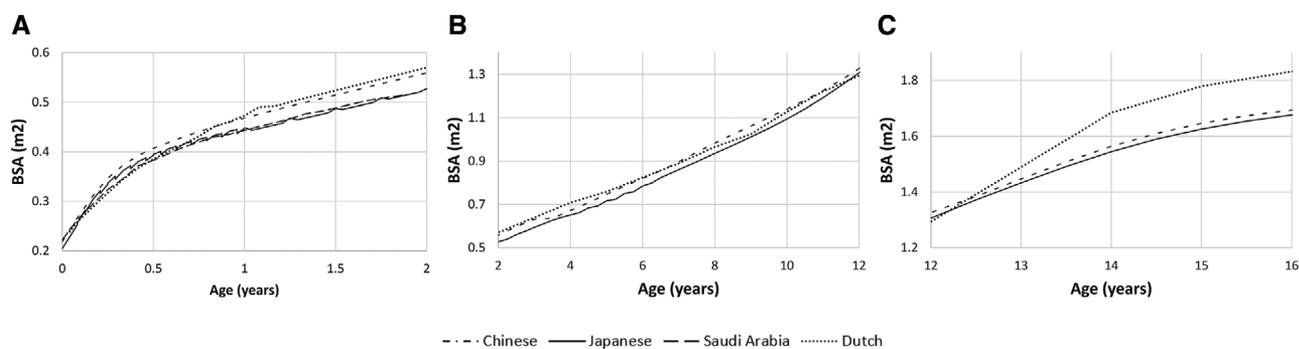
Figure 5. Comparison of BSA (m²) versus age in children from different countries: (A) birth-2 years, (B) 2-12 years, (C) 12-16 years. BSA was calculated using Haycock et al (1978) for BW below 15 kg and Du Bois and Du Bois (1989) for BW over 15 kg.
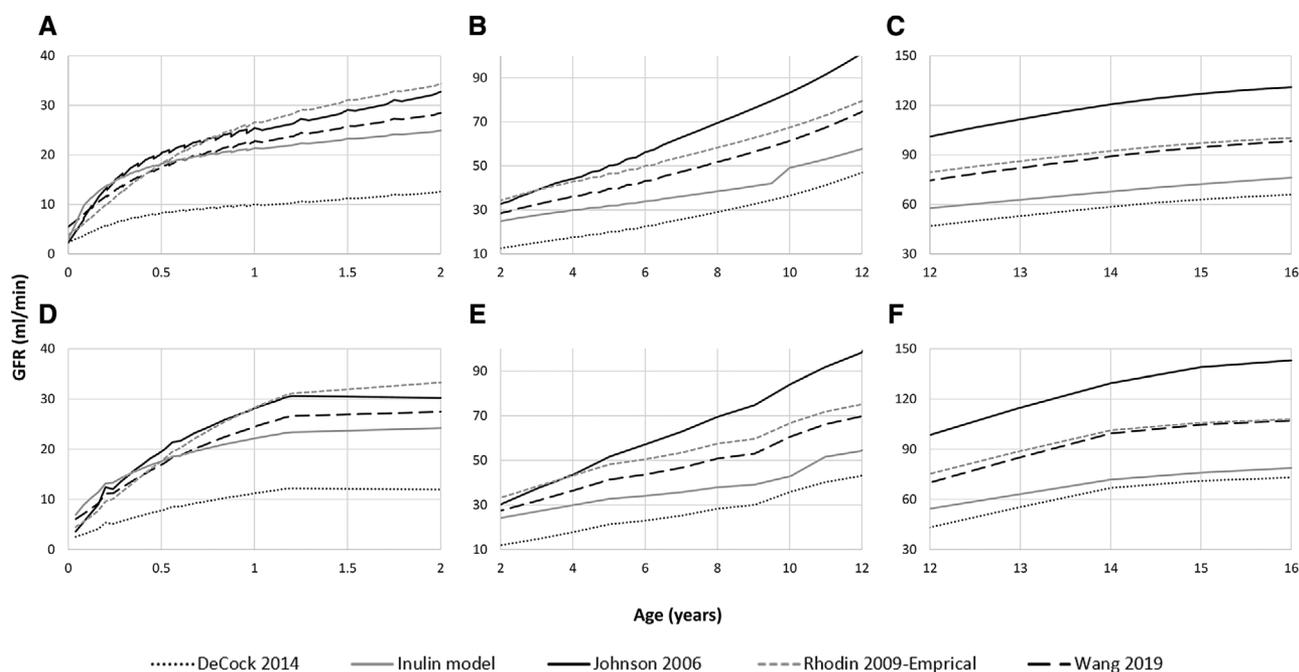
Figure 6. Predicted average GFR (mL/min) values in Japanese (A–C) and Dutch (D–F) pediatric subjects using different GFR models from the literature.

closest agent to inulin in terms of GFR.[62] Gadobutrol is not approved for use in infants and neonates, and because of lack of data, the performance of inulin model could not be evaluated in subjects younger than 2 years for this drug. Another potential factor contributing to this departure might be higher urine pH in metabolic acidosis of preterm neonates because of immaturity of ion transporters in early days that affects the ionization and excretion of these drugs.[63] Also, in our model, unlike Troutman et al,[39] we have included height as a pure function of postmenstrual age, which does not account for gestational age at birth of individuals in the model. The changes in height and weight for these preterm babies might be different from those growing inside the womb and might be another contributing factor to this departure.

Filtration of drugs is affected by the fraction unbound (fu) and renal blood flow.[64] Inulin is considered completely unbound in plasma, and therefore, binding covariates were not modeled. For the tested drugs, however, applying an fu correction to adult and pediatric clearance values would improve the predictions especially in preterm neonates; however, this was outside the scope of this study.

The pediatric clinical data are mainly from critically ill patients, which can impact the pharmacokinetics of drugs. To account for this effect to some extent, the clearance data from adult sepsis patients with normal renal function were used instead of clearance values from healthy adult volunteers. It is not clear, however, whether the renal function in some of these preterm neonates was normal, and it is not clear if the diseased

state could differ between adults and preterm neonates. For example, for the renin-angiotensin system that regulates urine output to maintain fluids and blood pressure shows higher plasma renin activity in preterm compared with full-term neonates.[65]

When comparing the models that use or do not use size as covariates, the difference in anthropometric measurements should be considered, and comparison should be made under different scenarios. Our simulation results demonstrated that GFR predictions (vs age) using various models in the literature will have different relative values depending on the study population and age-covariate relationship in that population. These relative differences are more pronounced in younger children. This comparison will require an independent data set for a compound that is purely filtered in glomeruli and known anthropometric measures of the population.

Conclusion

Age-dependent "active secretion" limits creatinine use as a pure measure of GFR ontogeny. A GFR ontogeny model is built using inulin data, avoiding the impact of active secretion. The model shows that birth has an impact on GFR value, and neonates with the same postmenstrual age who have been outside the womb longer have higher GFR values compared with more birth mature but younger neonates (with the same postmenstrual age but shorter postnatal age). Prenatal and postnatal GFR trajectories were distinguished. This difference should be considered when renally cleared drugs are administered to preterm neonates of different gestational and postnatal ages. Application of the GFR model to some renally cleared drugs tested shows a departure from systemic clearance for these drugs, indicating involvement of other mechanisms in addition to GFR in the clearance of these drugs.

Acknowledgments

Conflicts of Interest

F.S. and T.N.J. are employed full-time and A.B.J.H. and A.R.H. part-time by Certara, a company that develops and supplies modeling and simulation software and services to the pharmaceutical industry. A.R.H. is also director of the Centre for Applied Pharmacokinetic Research at the University of Manchester.

Data Accessibility Statement

For access to the data, please contact Dr Farzaneh Salem (farzaneh.salem@certara.com).

References

1. Allegaert K, Anderson BJ, Cossey V, Holford NH. Limited predictability of amikacin clearance in extreme premature neonates at birth. *Br J Clin Pharmacol*. 2006;61(1):39-48.
2. Allegaert K, Scheers I, Cossey V, Anderson BJ. Covariates of amikacin clearance in neonates: the impact of postnatal age on predictability. *Drug Metab Lett*. 2008;2(4):286-289.
3. Sherwin CM, Svahn S, Van der Linden A, Broadbent RS, Medlicott NJ, Reith DM. Individualised dosing of amikacin in neonates: a pharmacokinetic/pharmacodynamic analysis. *Eur J Clin Pharmacol*. 2009;65(7):705-713.
4. Botha JH, du Preez MJ, Adhikari M. Population pharmacokinetics of gentamicin in South African newborns. *Eur J Clin Pharmacol*. 2003;59(10):755-759.
5. DiCenzo R, Forrest A, Slish JC, Cole C, Guillet R. A gentamicin pharmacokinetic population model and once-daily dosing algorithm for neonates. *Pharmacotherapy*. 2003;23(5):585-591.
6. Garcia B, Barcia E, Perez F, Molina IT. Population pharmacokinetics of gentamicin in premature newborns. *J Antimicrob Chemother*. 2006;58(2):372-379.
7. Jensen PD, Edgren BE, Brundage RC. Population pharmacokinetics of gentamicin in neonates using a nonlinear, mixed-effects model. *Pharmacotherapy*. 1992;12(3):178-182.
8. Lanao JM, Calvo MV, Mesa JA, et al. Pharmacokinetic basis for the use of extended interval dosage regimens of gentamicin in neonates. *J Antimicrob Chemother*. 2004;54(1):193-198.
9. Nielsen EI, Sandstrom M, Honore PH, Ewald U, Friberg LE. Developmental pharmacokinetics of gentamicin in preterm and term neonates: population modelling of a prospective study. *Clin Pharmacokinet*. 2009;48(4):253-263.
10. Capparelli EV, Lane JR, Romanowski GL, et al. The influences of renal function and maturation on vancomycin elimination in newborns and infants. *J Clin Pharmacol*. 2001;41(9):927-934.
11. De Cock RF, Allegaert K, Brussee JM, et al. Simultaneous pharmacokinetic modeling of gentamicin, tobramycin and vancomycin clearance from neonates to adults: towards a semi-physiological function for maturation in glomerular filtration. *Pharm Res*. 2014;31(10):2643-2654.
12. Anderson BJ, Allegaert K, Van den Anker JN, Cossey V, Holford NH. Vancomycin pharmacokinetics in preterm neonates and the prediction of adult clearance. *Br J Clin Pharmacol*. 2007;63(1):75-84.
13. Kimura T, Sunakawa K, Matsuura N, Kubo H, Shimada S, Yago K. Population pharmacokinetics of arbekacin, vancomycin, and panipenem in neonates. *Antimicrob Agents Chemother*. 2004;48(4):1159-1167.
14. Rhodin MM, Anderson BJ, Peters AM, et al. Human renal function maturation: a quantitative description using weight and postmenstrual age. *Pediatr Nephrol*. 2009;24(1):67-76.
15. Fattinger K, Vozeh S, Olafsson A, Vlcek J, Wenk M, Follath F. Netilmicin in the neonate: population pharmacokinetic analysis and dosing recommendations. *Clin Pharmacol Ther*. 1991;50(1):55-65.
16. Fuchs A, Guidi M, Giannoni E, et al. Population pharmacokinetic study of gentamicin in a large cohort of premature and term neonates. *Br J Clin Pharmacol*. 2014;78(5):1090-1101.
17. Pullen J, Stolk LM, Nieman FH, Degraeuwe PL, van Tiel FH, Zimmermann LJ. Population pharmacokinetics and dosing of amoxicillin in (pre)term neonates. *Ther Drug Monit*. 2006;28(2):226-231.
18. Koteff J, Borland J, Chen S, et al. A phase 1 study to evaluate the effect of dolutegravir on renal function via measurement of iohexol and para-aminohippurate clearance in healthy subjects. *Br J Clin Pharmacol*. 2013;75(4):990-996.

19. Urakami Y, Kimura N, Okuda M, Inui K. Creatinine transport by basolateral organic cation transporter hOCT2 in the human kidney. *Pharm Res*. 2004;21(6):976-981.

20. Imamura Y, Murayama N, Okudaira N, et al. Prediction of fluoroquinolone-induced elevation in serum creatinine levels: a case of drug-endogenous substance interaction involving the inhibition of renal secretion. *Clin Pharmacol Ther*. 2011;89(1):81-88.

21. Lepist EI, Zhang X, Hao J, et al. Contribution of the organic anion transporter OAT2 to the renal active tubular secretion of creatinine and mechanism for serum creatinine elevations caused by cobicistat. *Kidney Int*. 2014;86(2):350-357.

22. Scotcher D, Arya V, Yang X, et al. A novel physiologically based model of creatinine renal disposition to integrate current knowledge of systems parameters and clinical observations. *CPT Pharmacometrics Syst Pharmacol*. 2020;9(6):310-321.

23. Scotcher D, Arya V, Yang X, et al. Mechanistic models as framework for understanding biomarker disposition: prediction of creatinine-drug interactions. *CPT Pharmacometrics Syst Pharmacol*. 2020;9(5):282-293.

24. Tanihara Y, Masuda S, Sato T, Katsura T, Ogawa O, Inui K. Substrate specificity of MATE1 and MATE2-K, human multidrug and toxin extrusions/H(+)-organic cation antiporters. *Biochem Pharmacol*. 2007;74(2):359-371.

25. Cheung KWK, van Groen BD, Spaans E, et al. A comprehensive analysis of ontogeny of renal drug transporters: mRNA analyses, quantitative proteomics, and localization. *Clin Pharmacol Ther*. 2019;106(5):1083-1092.

26. Li CY, Hosey-Cojocari C, Basit A, Unadkat JD, Leeder JS, Prasad B. Optimized renal transporter quantification by using aquaporin 1 and aquaporin 2 as anatomical markers: application in characterizing the ontogeny of renal transporters and its correlation with hepatic transporters in paired human samples. *AAPS J*. 2019;21(5):88.

27. Filler G, Yasin A, Medeiros M. Methods of assessing renal function. *Pediatr Nephrol*. 2014;29(2):183-192.

28. Johnson TN, Rostami-Hodjegan A, Tucker GT. Prediction of the clearance of eleven drugs and associated variability in neonates, infants and children. *Clin Pharmacokinet*. 2006;45(9):931-956.

29. Wang J, Kumar SS, Sherwin CM, et al. Renal clearance in newborns and infants: predictive performance of population-based modeling for drug development. *Clin Pharmacol Ther*. 2019;105(6):1462-1470.

30. Abduljalil K, Pan X, Pansari A, Jamei M, Johnson TN. A preterm physiologically based pharmacokinetic model. Part I: physiological parameters and model building. *Clin Pharmacokinet*. 2019;59(4):485-500.

31. Haycock GB, Schwartz GJ, Wisotsky DH. Geometric method for measuring body surface area: a height-weight formula validated in infants, children, and adults. *J Pediatr*. 1978;93(1):62-66.

32. Du Bois D, Du Bois EF. A formula to estimate the approximate surface area if height and weight be known. 1916. *Nutrition*. 1989;5(5):303-311.

33. Meban C. The surface area and volume of the human fetus. *J Anat*. 1983;137(Pt 2):271-278.

34. Bauer LA, Blouin RA. Gentamicin pharmacokinetics: effect of aging in patients with normal renal function. *J Am Geriatr Soc*. 1982;30(5):309-311.

35. Dickson CJ, Schwartzman MS, Bertino JS, Jr. Factors affecting aminoglycoside disposition: effects of circadian rhythm and dietary protein intake on gentamicin pharmacokinetics. *Clin Pharmacol Ther*. 1986;39(3):325-328.

36. Rotschafer JC, Crossley K, Zaske DE, Mead K, Sawchuk RJ, Solem LD. Pharmacokinetics of vancomycin: observations in 28 patients and dosage recommendations. *Antimicrob Agents Chemother*. 1982;22(3):391-394.

37. Barbhaiya RH, Knupp CA, Pfeffer M, Pittman KA. Lack of pharmacokinetic interaction between cefepime and amikacin in humans. *Antimicrob Agents Chemother*. 1992;36(7):1382-1386.

38. Clarke JT, Libke RD, Regamey C, Kirby WM. Comparative pharmacokinetics of amikacin and kanamycin. *Clin Pharmacol Ther*. 1974;15(6):610-616.

39. Troutman JA, Sullivan MC, Carr GJ, Fisher J. Development of growth equations from longitudinal studies of body weight and height in the full term and preterm neonate: From birth to four years postnatal age. *Birth Defects Res*. 2018;110(11):916-932.

40. Davies DF, Shock NW. Age changes in glomerular filtration rate, effective renal plasma flow, and tubular excretory capacity in adult males. *J Clin Invest*. 1950;29(5):496-507.

41. Pierrat A, Gravier E, Saunders C, et al. Predicting GFR in children and adults: a comparison of the Cockcroft-Gault, Schwartz, and modification of diet in renal disease formulas. *Kidney Int*. 2003;64(4):1425-1436.

42. Prescott LF, Freestone S, McAuslane JA. Reassessment of the single intravenous injection method with inulin for measurement of the glomerular filtration rate in man. *Clin Sci (Lond)*. 1991;80(2):167-176.

43. Eisner C, Faulhaber-Walter R, Wang Y, et al. Major contribution of tubular secretion to creatinine clearance in mice. *Kidney Int*. 2010;77(6):519-526.

44. Soveri I, Berg UB, Bjork J, et al. Measuring GFR: a systematic review. *Am J Kidney Dis*. 2014;64(3):411-424.

45. Golper TA, Noonan HM, Elzinga L, et al. Vancomycin pharmacokinetics, renal handling, and nonrenal clearances in normal human subjects. *Clin Pharmacol Ther*. 1988;43(5):565-570.

46. Dean RF, McCance RA. Inulin, diodone, creatinine and urea clearances in newborn infants. *J Physiol*. 1947;106(4):431-439.

47. Doxiadis SA, Goldfinch MK. Comparison of inulin and endogenous creatinine clearance in young children. *J Physiol*. 1952;118(4):454-460.

48. Sterner G, Frennby B, Mansson S, Nyman U, Van Westen D, Almen T. Determining 'true' glomerular filtration rate in healthy adults using infusion of inulin and comparing it with values obtained using other clearance techniques or prediction equations. *Scand J Urol Nephrol*. 2008;42(3):278-285.

49. Bartelink IH, Rademaker CM, Schobben AF, van den Anker JN. Guidelines on paediatric dosing on the basis of developmental physiology and pharmacokinetic considerations. *Clin Pharmacokinet*. 2006;45(11):1077-1097.

50. StatPearls. Treasure Island, FL: StatPearls Publishing. https://www.ncbi.nlm.nih.gov/books/NBK430685/. Published 2020. Accessed June 1, 2020.

51. Vrancken SL, van Heijst AF, de Boode WP. Neonatal hemodynamics: from developmental physiology to comprehensive monitoring. *Front Pediatr*. 2018;6:87.

52. Currie BP, Lemos-Filho L. Evidence for biliary excretion of vancomycin into stool during intravenous therapy: potential implications for rectal colonization with vancomycin-resistant enterococci. *Antimicrob Agents Chemother*. 2004;48(11):4427-4429.

53. Matzke GR, Zhanel GG, Guay DR. Clinical pharmacokinetics of vancomycin. *Clin Pharmacokinet*. 1986;11(4):257-282.

54. Hori Y, Aoki N, Kuwahara S, et al. Megalin blockade with cilastatin suppresses drug-induced nephrotoxicity. *J Am Soc Nephrol*. 2017;28(6):1783-1791.

55. Zaric RZ, Milovanovic J, Rosic N, et al. Pharmacokinetics of vancomycin in patients with different renal function levels. *Open Med (Wars)*. 2018;13(1):512-519.

56. Nakamura T, Takano M, Yasuhara M, Inui K. In-vivo clearance study of vancomycin in rats. *J Pharm Pharmacol*. 1996;48(11):1197-1200.

57. Nivoche Y, Contrepois A, Cremieux AC, Carbon C. Vancomycin in rabbits: pharmacokinetics, extravascular diffusion, renal excretion and interactions with furosemide. *J Pharmacol Exp Ther*. 1982;222(1):237-240.

58. Sokol PP. Mechanism of vancomycin transport in the kidney: studies in rabbit renal brush border and basolateral membrane vesicles. *J Pharmacol Exp Ther*. 1991;259(3):1283-1287.

59. Brion N, Barge J, Godefroy I, et al. Gentamicin, netilmicin, dibekacin, and amikacin nephrotoxicity and its relationship to tubular reabsorption in rabbits. *Antimicrob Agents Chemother*. 1984;25(2):168-172.

60. Contrepois A, Brion N, Garaud JJ, et al. Renal disposition of gentamicin, dibekacin, tobramycin, netilmicin, and amikacin in humans. *Antimicrob Agents Chemother*. 1985;27(4):520-524.

61. Te Brake LH, van den Heuvel JJ, Buaben AO, et al. Moxifloxacin is a potent in vitro inhibitor of OCT- and MATE-mediated transport of metformin and ethambutol. *Antimicrob Agents Chemother*. 2016;60(12):7105-7114.

62. US Food and Drug Administration, The Center for Drug Evaluation and Research. Application number 201277Orig1s000: summary review. https://www.accessdata.fda.gov/drugsatfda_docs/nda/2011/201277Orig1s000SumR.pdf. Accessed July 11, 2019.

63. Sato T, Takahashi N, Komatsu Y, et al. Urinary acidification in extremely low birth weight infants. *Early Hum Dev*. 2002;70(1-2):15-24.

64. Cristea S, Krekels EHJ, Allegaert K, Knibbe CAJ. The predictive value of glomerular filtration rate-based scaling of pediatric clearance and doses for drugs eliminated by glomerular filtration with varying protein-binding properties. *Clin Pharmacokinet*. 2020; doi: https://doi.org/10.1007/s40262-020-00890-2.

65. Sulyok E, Nemeth M, Tenyi I, et al. Relationship between maturity, electrolyte balance and the function of the renin-angiotensin-aldosterone system in newborn infants. *Biol Neonate*. 1979;35(1-2):60-65.

Supplemental Information

Additional supplemental information can be found by clicking the Supplements link in the PDF toolbar or the Supplemental Information section at the end of web-based version of this article.